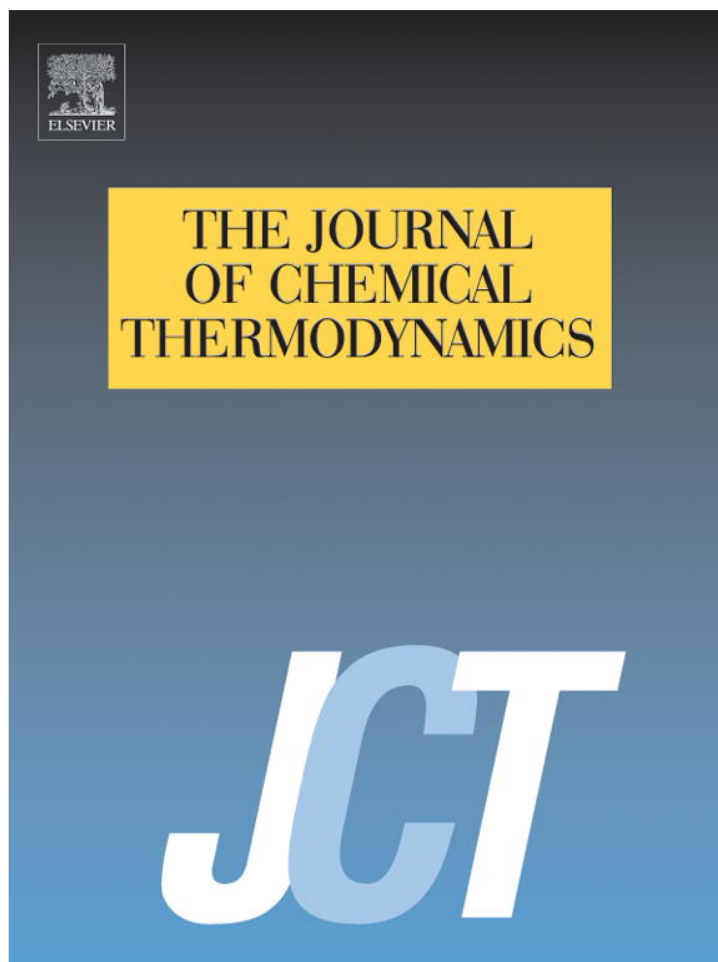


Provided for non-commercial research and education use.  
Not for reproduction, distribution or commercial use.



(This is a sample cover image for this issue. The actual cover is not yet available at this time.)

**This article appeared in a journal published by Elsevier. The attached copy is furnished to the author for internal non-commercial research and education use, including for instruction at the authors institution and sharing with colleagues.**

**Other uses, including reproduction and distribution, or selling or licensing copies, or posting to personal, institutional or third party websites are prohibited.**

**In most cases authors are permitted to post their version of the article (e.g. in Word or Tex form) to their personal website or institutional repository. Authors requiring further information regarding Elsevier's archiving and manuscript policies are encouraged to visit:**

**<http://www.elsevier.com/copyright>**



Contents lists available at SciVerse ScienceDirect

J. Chem. Thermodynamics

journal homepage: [www.elsevier.com/locate/jct](http://www.elsevier.com/locate/jct)

## On isentropic lines and isentropic exponents

Kandadai Srinivasan<sup>a,1</sup>, Pradip Dutta<sup>a</sup>, Santiago Velasco<sup>b</sup>, Juan A. White<sup>b,\*</sup>

<sup>a</sup> Department of Mechanical Engineering, Indian Institute of Science, Bangalore 560 012, India

<sup>b</sup> Departamento de Física Aplicada, Universidad de Salamanca, 37008 Salamanca, Spain

### ARTICLE INFO

#### Article history:

Received 25 April 2012

Received in revised form 9 July 2012

Accepted 13 July 2012

Available online 22 July 2012

#### Keywords:

Isentropic lines

Sound speed

Isentropic index

### ABSTRACT

The three indicators of isentropic lines, namely, the isentropic index, the ratio of pressure and density  $p/\rho$  and the derivative  $(\partial p/\partial \rho)_s$ , are investigated for all of the fluids in the RefProp 9.0 program. The behaviour of these three entities is evaluated along the saturated vapour line as well as in the superheated vapour region. There is a distinct demarcation of fluids whose isentropic indices can be less than 1 and others for which this behaviour is absent. The critical molar volume is found to be the characterizing feature. Several other interesting features of those three thermodynamic properties are also highlighted. It is observed that most practical engineering compression and expansion processes occur along the decreasing direction of the sound speed.

© 2012 Elsevier Ltd. All rights reserved.

### 1. Introduction

The chart depicting thermodynamic properties of fluids in the natural logarithm of pressure – enthalpy ( $\ln p$  vs  $h$ ) coordinate system is amongst the most widely used for analysis of refrigeration, heat pumping and Rankine cycle systems. The behaviour of isentropes, isochores and isotherms in this plane provides an insight to engineering limits of operation of those cycles. For example, thermodynamic cycles are seldom operated close to the triple point or close to the critical point of a fluid. Srinivasan [1] pointed out that most systems are operated within the pressure limits corresponding to where maxima in  $p_r(1 - T_r)$  and  $T_r(1 - p_r)$  occur along the saturation line, with  $p_r$  and  $T_r$  being reduced pressure and temperature, respectively. The transcritical carbon dioxide refrigeration cycle is a peculiar exception where actually the cycle is operated in the negative slope region of saturated enthalpy on the  $\ln p$ – $h$  plane [2].

The curvature of isentropes on  $p$ – $h$  and  $\ln p$ – $h$  planes has been discussed by Bisio and Martini [3] for isentropic compressions for ideal and real fluids. When one considers the standard vapour compression refrigeration cycle, the energy input which is made imminent from Second Law of thermodynamics occurs during the isentropic compression process. Industry also attempts to perform the isentropic process but only with limited success because most refrigeration compressors available in the market have isentropic efficiency seldom exceeding 80% while the most common

range is 55% to 65% [4]. Taras and Lifson [5] point out that fluids with steeper isentropes are generally associated with higher isentropic efficiencies. On the other hand, a large impetus is being given to “green” power which opens the option of concentrated solar thermal power using working fluids that have low global warming potential. In addition, choosing an appropriate working fluid for low grade industrial waste heat recovery using small capacity (of the order of 10’s of kW) organic Rankine cycles is also fraught with low isentropic efficiencies of expanders. It appears that raising this figure to above 75% is a technological problem [6,7]. It is imperative that any paradigm boost of isentropic efficiency of the expander contributes to reduction in the size of the solar field and the unit cost of electricity generated. In this background it is worthwhile investigating the nature of isentropes originating from various states along the saturated vapour line of various working fluids and extending into superheated vapour region and assessing their relevance to the above mentioned cycles. Isentropes are also useful in analysing shock phenomena and sudden changes in the gas flow domains. For example, smooth loss of convexity of isentropes has been a topic of interest [8,9].

### 2. Indicators of isentropic lines in the vapour region

Starting from the definition of specific enthalpy

$$h = u + pv, \quad (1)$$

the basic thermodynamic relation

$$dh = T ds + v dp \quad (2)$$

implies that

$$(\partial p/\partial h)_s = 1/v = \rho, \quad (3)$$

\* Corresponding author. Address: IUFFyM, Universidad de Salamanca, 37008 Salamanca, Spain. Tel.: +34 923294436; fax: +34 923294584.

E-mail address: [white@usal.es](mailto:white@usal.es) (J.A. White).

<sup>1</sup> Also with Department of Mechanical Engineering, University of Melbourne, Australia.

and therefore, in a simple  $p$ – $h$  plane the isentrope should be concave with reference to the ordinate because any compression must result in an increase in density and any expansion must result in a decrease in density. Invariably all working fluids used in current engineering practice depict this feature.

However, most engineering charts depict a  $\ln p$ – $h$  relation wherein the slope of the isentrope is not that obvious. More concretely, one has

$$(\partial \ln p / \partial h)_s = \rho / p, \quad (4)$$

and consequently, the nature of the right hand side of the above equation determines the behaviour of an isentrope in the  $\ln p$ – $h$  plane. The interesting feature is that, along an isentrope, unlike the density,  $\rho/p$  is not necessarily monotonic. We have found that  $\rho/p$  along an isentrope is monotonic for some fluids and for many others it has a minimum and a maximum. In this work we shall investigate the criteria that demarcate this behaviour.

Two other thermodynamic properties associated with constant entropy are the sound speed defined as

$$c = \{(\partial p / \partial \rho)_s\}^{1/2}, \quad (5)$$

and the isentropic coefficient defined as

$$k = (\partial \ln p / \partial \ln \rho)_s, \quad (6)$$

from which it also follows that

$$c = \{k(p/\rho)_s\}^{1/2}. \quad (7)$$

Thus, we have three properties that characterise an isentrope, namely,  $c$ ,  $k$  and  $(p/\rho)_s$ , each of which is found to depict an interesting fluid specific behaviour. The objective of this paper is also to analyse conditions related to those indicators of the isentropes.

In this paper, we have used all of the fluids included in the NIST program RefProp 9.0 [10] for all of the property evaluations. We consider only a few of them to demonstrate the key features mentioned earlier. Hydrogen, helium and neon are not considered because of quantum effects and also since several features common to other fluids do not occur for them.

### 3. Fluid specific behaviour of isentrope indicators

Figures 1 and 2 show the pressure dependence of each of the three properties for two representative fluids namely propane and ammonia along an isentrope corresponding to saturated vapour at 1.013 bar. In these figures, for the sake of comparison, the saturated vapour state values are also plotted. In figure 1 the left ordinate for sound speed is  $c/4$  to bring the order of magnitude to be the same as for  $p/\rho$  to enable discussion hereafter.

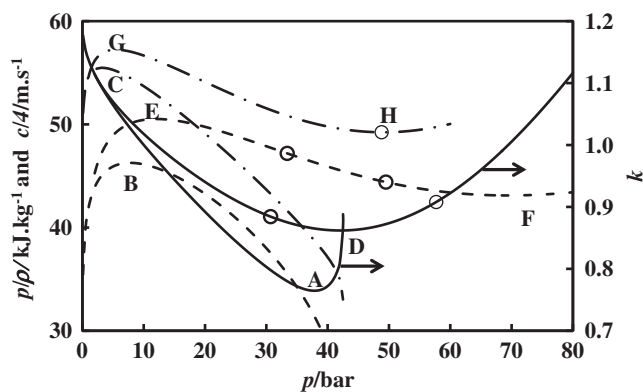


**FIGURE 1.** Pressure ( $p$ ) dependence of  $c$ ,  $p/\rho$  and  $k$  for propane. Legend: solid line,  $k$  (right ordinate); ----,  $p/\rho$  (left ordinate); -·-·-,  $c/4$  (left ordinate). Lines with O, saturated vapour isentrope at 1.013 bar. Lines without markers: saturated vapour.

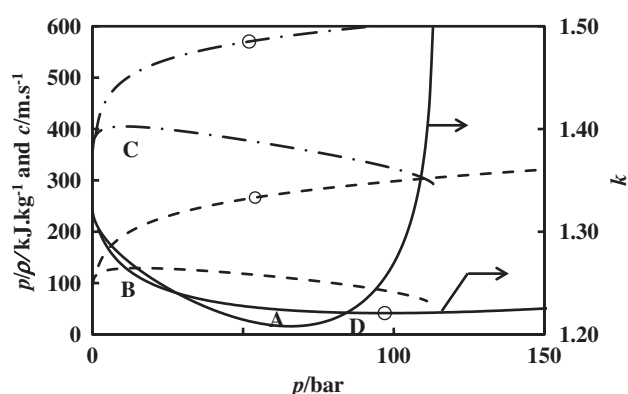


**FIGURE 2.** Pressure ( $p$ ) dependence of  $c$ ,  $p/\rho$  and  $k$  for ammonia. Legend: solid line,  $k$  (right ordinate); ----,  $p/\rho$  (left ordinate); -·-·-,  $c/4$  (left ordinate). Lines with O, saturated vapour isentrope at 1.013 bar. Lines without markers: saturated vapour.

Common features for both fluids in the saturated vapour state are: (a) a minimum in the isentropic coefficient at a particular pressure (A in figures 1 and 2), (b) a maximum in  $p/\rho$  at another pressure (B in figures 1 and 2), (c) a maximum in the sound speed at yet another pressure (C in figures 1 and 2). In the superheated state also the isentropic coefficient has a minimum at yet another pressure along the isentrope corresponding to saturation vapour state at 1.013 bar (D in figures 1 and 2). However, the differences between propane and ammonia are: (a)  $p/\rho$  has one maximum (E in figure 1) and one minimum pressure (F in figure 1) and (b) the sound speed has a maximum and a minimum along the isentrope through saturated vapour at 1.013 bar (G and H in figure 1) of propane which is absent in the case of ammonia.

When  $p/\rho$  has a maximum or a minimum along an isentrope, this implies that at these points

$$[\partial(p/\rho)/\partial p]_s = 0, \quad (8)$$

and hence

$$[\partial p / \partial \rho]_s = p / \rho. \quad (9)$$

From which it also follows that, at these points, from equation (6)  $k = 1$  and from equation (7),  $c = \{(p/\rho)_s\}^{1/2}$ .

In the case of propane, this also implies that  $k < 1$  between these pressures of extrema along an isentrope (between  $p_E$  and  $p_F$  in figure 1). Further, along the saturated vapour line, in the case of propane  $k < 1$  for  $p > 10$  bar, whereas in the case of ammonia  $k > 1$  at all states. It is evident that the popular concept of isentropic coefficient being approximated to the ratio of specific heats cannot be applied to real gases and they are separate entities because the isobaric specific heat,  $c_p$  cannot be less than the isochoric specific heat,  $c_v$  whereas  $k$  can be less than 1 as seen above.

In the case of the saturated vapour state of propane, the pressure at which the maximum in  $p/\rho_g$  (where the subscript  $g$  refers to the saturated vapour state) occurs (B in figure 1) is  $\sim 8$  bar and is not the same as the pressure at which  $k_g = 1$  which is  $\sim 10$  bar. This is because equation (9) requires the gradient along an isentrope whereas point B is along the saturation line. The loci of pressures of maximum (E in figure 1) and minimum (F in figure 1) in  $p/\rho$  along various isentropes for propane are shown in figures 3 and 4 respectively. It is apparent that the isentropes corresponding to the saturated vapour state where  $k_g < 1$  will not have a maximum in  $p/\rho$  and hence the limiting saturation pressure in figure 3 is 10.02 bar. Above this saturation pressure only a minimum in  $p/\rho$  will exist whose locus is shown in figure 4. Obviously, such behaviour will not happen for ammonia since  $p/\rho$  for this fluid is monotonic. Figure 4 also shows the trace of pressures at which  $k_{min}$

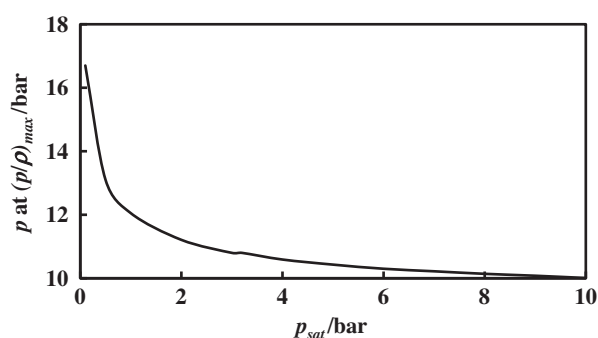


FIGURE 3. Trace of pressure ( $p$ ) at  $(p/\rho)_{max}$  (locus of point E in figure 1) for propane isentropes originating from the saturated vapour state ( $p_{sat}$ ).

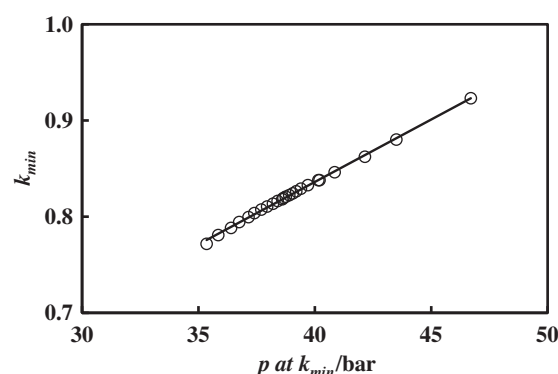


FIGURE 6.  $k_{min}$  along the isentropes in the superheated region of propane vs the pressure where it occurs.

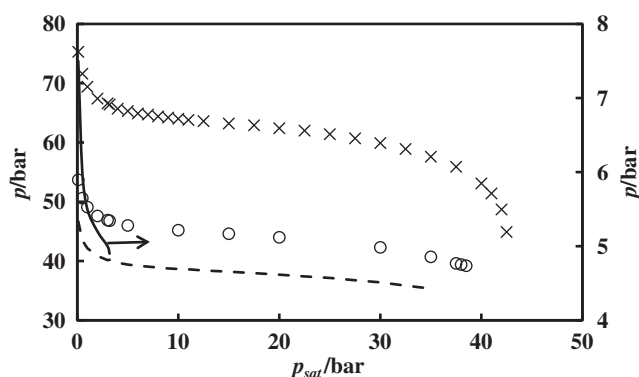


FIGURE 4. Loci of pressures at extrema along isentropes through saturated state of propane vapour. Legend: X, for  $(p/\rho)_{min}$ ; O, for  $c_{min}$ ; ----, for  $k_{min}$ ; solid line, for  $c_{max}$  (right ordinate).

occurs along each isentrope in the superheated state. Such a trace will exist even for ammonia.

Figure 5 shows a trace of pressures at which  $k_{min}$  occurs and its value for various isentropes through the saturated vapour state (designated by the saturated pressures) (point D in figures 1 and 2) for propane and ammonia. For either of these fluids the existence of  $k_{min}$  is only up to isentropes through 40 bar, beyond which it is monotonic. Although, the range of variation of  $k_{min}$  in the case of ammonia is not even 2%, it is much larger in the case of propane. On the other hand there is a larger variation in the pressures of occurrence of  $k_{min}$  for ammonia than for propane.

Figure 6 shows the relation between the values of  $k_{min}$  along various isentropes in the superheated state and the pressures at

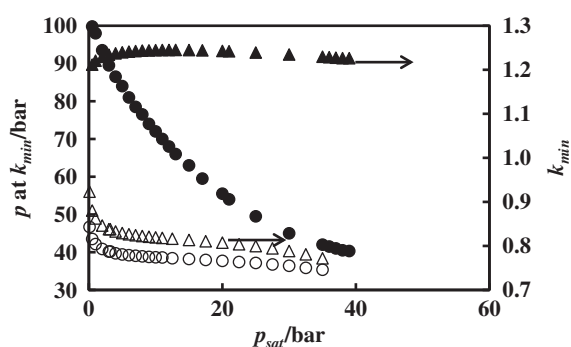


FIGURE 5. Trace of pressures at which  $k_{min}$  occurs (left ordinate) and its value (right ordinate) along various isentropes through the saturated vapour state. Legend ●,  $p$  at  $k_{min}$  ammonia; ▲,  $k_{min}$  ammonia; O,  $p$  at  $k_{min}$  propane; and △,  $k_{min}$  propane.

which they occur for propane. A good linear relation exists between  $k_{min}$  and the pressure where it occurs for propane as given below

$$K_{min} = 0.013 + 0.3166(p/\text{bar}) \text{ for } 35 < p/\text{bar} < 50 \quad (10)$$

with a regression coefficient of 0.9986. Similar relations can be obtained for other fluids as well.

#### 4. Behaviour along the saturated vapour line

In this section, we will analyse the behaviour of the three indicators of the isentropes, namely  $c_{gmax}$ ,  $k_{gmin}$ , and  $(p/\rho_g)_{max}$  along the saturated vapour line for the fluids included in RefProp 9.0. Figure 7 shows the acentric factor ( $\omega$ ) dependence of the reduced temperatures ( $T/T_c$ ) at which those extrema occur. In general, the occurrence of  $k_{gmin}$  is within 10% of the critical temperature for a large majority of fluids with  $\omega > 0.2$ . The point of occurrence of  $(p/\rho_g)_{max}$  seems to be nearly independent of the acentric factor. A maximum reduced temperature of 0.82 occurs for methylenolene ( $\omega = 1.14$ ) and a minimum of 0.77 for R41 ( $\omega = 0.2$ ). In fact, the mean reduced temperature for all fluids is 0.788 with a standard deviation of 0.009. It is worthwhile noting that the reduced temperature at which  $c_{gmax}$  occurs decreases with increase in the acentric factor of up to about  $\omega \sim 0.2$  and then it increases linearly. The range of variation of the reduced temperature is between 0.82 and 0.68. It is also observed that most fluids that fall outside the broad pathway are inorganic fluids such as water (both normal and heavy), carbon dioxide, ammonia, sulphur dioxide, nitrous oxide, etc. Ethanol and methanol consistently fall outside the spectrum for reasons already brought out by Srinivasan *et al.* [11] and Velasco *et al.* [12].

The inter-relationship between the reduced saturated vapour density ( $\rho_g/\rho_c$ ) and the reduced pressure ( $p/p_c$ ) at which the extrema occur is shown in figure 8. Since a fair correlation is observed, the following least squares fits are obtained:

$$P_r \text{ at } (p/\rho_g)_{max} = 0.0378 + 1.893\rho_{gr} \quad (11)$$

with a regression coefficient of 0.9858

$$p_r \text{ at } c_{gmax} = 0.0081 + 2.165\rho_{gr} \quad (12)$$

with a regression coefficient of 0.9944

$$p_r \text{ at } k_{gmin} = 0.0066 + 2.252\rho_{gr} - 1.697\rho_{gr}^2 \quad (13)$$

with a regression coefficient of 0.9918.

It is also observed that the reduced density at which an extremum occurs along the saturated vapour line is well correlated with the magnitudes of the maxima themselves. This is shown in figure 9 where we plot  $k_{gmin}$ , the reduced maximum in  $(p/\rho_g)_{max}$  (defined

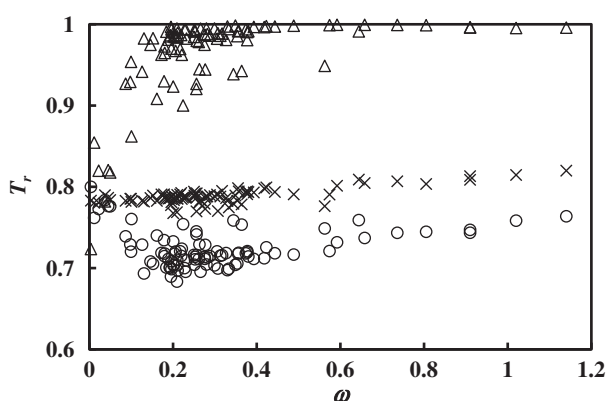


**FIGURE 7.** Saturated reduced temperatures ( $T_r$ ) at which extrema occur vs acentric factor ( $\omega$ ) for all of the fluids in RefProp 9.0. Legend:  $\Delta$ ,  $k_{gmin}$ ;  $X$ ,  $c_{gmax}$ ; and  $\circ$  -  $(p/\rho_g)_{max}$ .

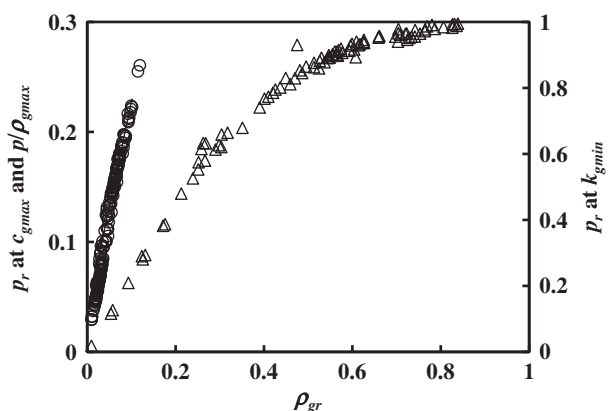


**FIGURE 8.** Saturated reduced pressures at which extrema occur vs reduced density. Legend:  $\Delta$ ,  $k_{gmin}$  (right ordinate);  $X$ ,  $c_{gmax}$ ; and  $\circ$  -  $(p/\rho_g)_{max}$ .

as  $(p_r/\rho_{gr})_{max}$ ) and the dimensionless sound speed  $c_{gmax} = c_{gmax}/\{(RT_c/M)\}^{1/2}$ , where  $R$  is the Universal gas constant and  $M$  is the molar mass.

From figure 9 one observes that,  $k_{gmin}$  and  $(p_r/\rho_{gr})_{max}$  are fairly well correlated against  $\rho_{gr}$ . We obtain the following empirical equations:

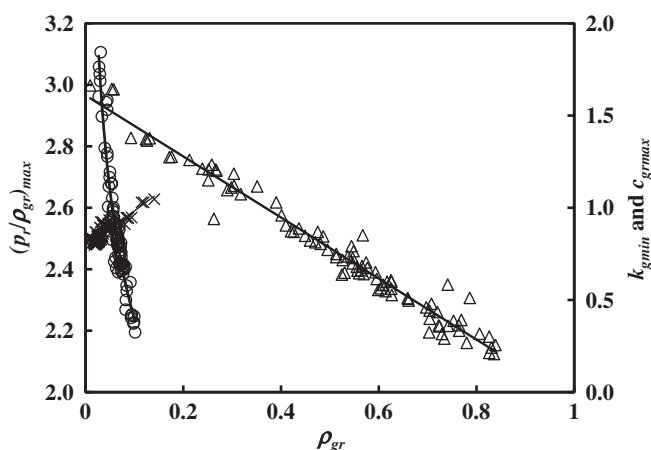


**FIGURE 9.** Reduced density ( $\rho_{gr}$ ) dependence of  $k_{gmin}$  ( $\Delta$ , right ordinate),  $c_{gmax}$  ( $\times$ , right ordinate), and  $(p_r/\rho_{gr})_{max}$  ( $\circ$ , left ordinate).

$$(p_r/\rho_{gr})_{max} = 1.263/\rho_{gr}^{0.248} \quad (14)$$

with a regression coefficient of 0.9011, and

$$k_{gmin} = 1.610 - 1.655\rho_{gr} \quad (15)$$

with a regression coefficient of 0.9687.

However, since  $c_{gmax}$  occurs over a narrow band of 0.8 to 1.04 and the trend is not systematic, no correlation has been obtained for this quantity.

We have found that the fluids with a critical volume less than  $0.15 \text{ m}^3 \cdot \text{kmol}^{-1}$  possess  $k_{gmin} > 1$  (see table S1 of the supplementary data). Most cryogenic liquids, low molecular weight hydrocarbons, inorganic fluids such as water, ammonia, carbon dioxide fall under this category. For fluids with critical volume larger than  $0.15 \text{ m}^3 \cdot \text{kmol}^{-1}$ ,  $k_{gmin} < 1$ . Most commercial organic refrigerants, high molecular weight hydrocarbons and organic compounds fall under this category. From figure 9 it is also seen that the former category of fluids for which  $k_{gmin} > 1$ ,  $\rho_{gr} < 0.39$  where  $k_{gmin}$  occurs. Broadly, fluids with  $k_{gmin} > 1$  do not show a maximum in  $(p/\rho)$  nor in  $c$  in the superheated region.

Except for fluorine, oxygen, nitrogen, argon, krypton, xenon, methane, carbon monoxide, and hydrogen sulphide, the rest of the fluids analysed attain  $k_{gmin}$  at  $T_r > 0.9$ , which is a region seldom considered for power and refrigeration applications. Water, carbon dioxide and ethylene were found to possess also a maximum in  $k_g$  along the saturated vapour line (figure 10). In this figure saturated vapour lines for ammonia and propane are drawn again to show the contrast. In the case of propane and ammonia,  $k_c$  at the critical point is large (but not infinite). The three parameters of the isentropes are finite at the critical point because  $[\partial p/\partial \rho]_s$  is finite although  $[\partial p/\partial \rho]_c$  is zero along the saturation line. Thus, the manifestation of critical isentrope of a fluid would govern this feature and this also is expected to be highly fluid dependent.

## 5. Thermodynamic planes with isentropic indicators and pressure

The generally accepted practice in representing thermodynamic planes is to use one intensive (usually the ordinate) and one extensive property per unit mass (usually the abscissa) (e.g.:  $p$ - $v$ ,  $T$ - $s$  diagrams) or two extensive properties (e.g.:  $h$ - $s$  diagram). According to Valentin and Balian [13] there is a substantial progress in the quality of data for the speed of sound and it can be used as an intensive property for representing thermodynamic diagrams. Perhaps, this could be the starting point of looking at thermodynamic diagrams with two intensive properties.

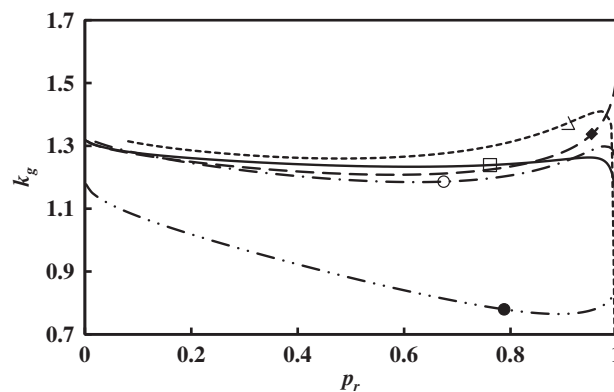


**FIGURE 10.** Saturated vapour lines on the  $k_g$ - $p$  plane. Legend:  $\Delta$ , carbon dioxide;  $\square$ , water;  $\circ$ , ethylene;  $\blacklozenge$ , ammonia; and  $\bullet$  - propane.

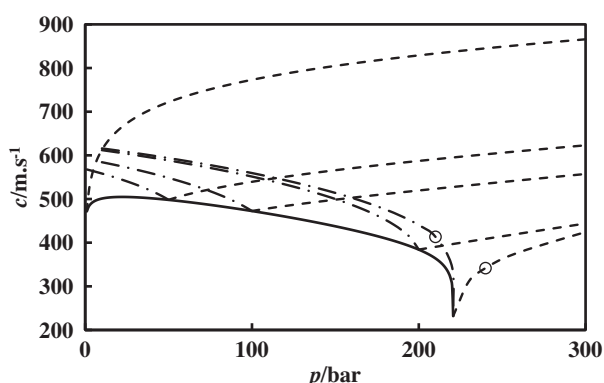


FIGURE 11. Sound speed ( $c$ )–pressure ( $p$ ) plane for water. Solid line, saturated vapour line, ----, isentropes, -.-.-, isotherms. ○– iso-lines through the critical point.

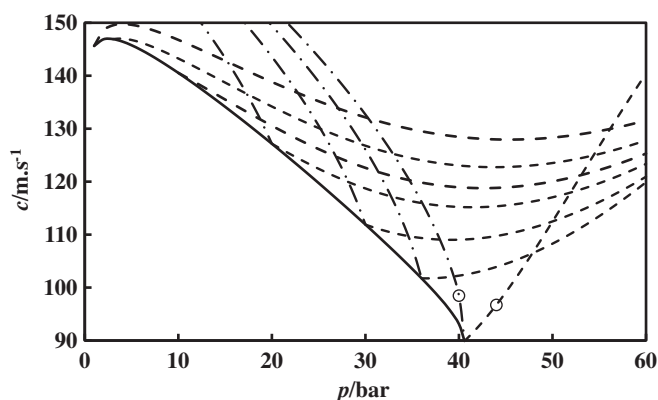


FIGURE 12. Sound speed ( $c$ )–pressure ( $p$ ) plane for HFC134a. Solid line, saturated vapour line, ----, isentropes, -.-.-, isotherms. ○– iso-lines through the critical point.

The foregoing findings can also be appreciated if the  $c$ – $p$  plane is used to describe the thermodynamic properties of fluids. We choose water and HFC 134a as two example fluids to demonstrate the nature of this plane. Each of them lies on either side of the demarcating critical molar volume of  $0.15 \text{ m}^3 \cdot \text{kmol}^{-1}$ . They are shown in figures 11 and 12 in which the saturated vapour and the isentropes in the superheated vapour zone are depicted.

The engineering implications of the above findings are as follows. The fluids used in refrigeration, if compressed from a state where the isentropic coefficient is less than 1 will undergo a slower increase in temperatures than those with higher isentropic coefficients. For example, this is the case when ammonia or carbon dioxide is used as a refrigerant where the discharge temperatures of a compressor are high and there is a large desuperheating zone or a large gas cooling requirement in the heat rejection process. This is associated with lubricating oil management problems. In practice, heat recovery hardware is sometimes added.

For a typical vapour compression refrigeration system using HFC 134a as the working fluid, the isentropic compression in practical limits of operation would be in the direction of decreasing sound speed of the process. Similarly, in the case of steam, which is a very good turbine expansion fluid, again the direction of expansion will be in the direction of decreasing sound speed. From a practicality point of view, it appears that the favourable direction of processes (compression or expansion) would be in the direction of decreasing sound speed along an isentrope.

It is also seen that  $k_{gmin}$  occurs for most fluids at  $T_r > 0.9$  where an engineering system is seldom operated (except CO<sub>2</sub> based systems). When newer refrigerants are synthesized, criteria described herein could enable prima facie evaluation of the compression process. For example, for the new refrigerant HFE143m [14], which has a critical volume of  $0.2151 \text{ m}^3 \cdot \text{kmol}^{-1}$ ,  $k_{gmin} \sim 0.716$  and will occur at  $\rho_{gr} = 0.54$  or  $\rho_g = 251 \text{ kg/m}^3$  where the saturation temperature is  $99.8 \text{ }^\circ\text{C}$  and the corresponding pressure is  $\sim 33 \text{ bar}$  which is quite close to the critical state. Thus, this refrigerant will be a reasonable replacement for HFC 134a, as expected. On the other hand, the search for newer environmentally friendly organic Rankine cycle working fluids can be assessed to satisfy the criterion of decreasing sound speed in the expander.

## 6. Summary

The three indicators of constant entropy lines are the isentropic index, the ratio of pressure and density and the sound speed. These three properties have systematic trends for all fluids along the saturated vapour curve, but have fluid specific behaviour in the superheated region. They have been analysed for all fluids under RefProp 9.0 and it is seen that the critical molar volume is the demarcating feature. Empirical correlations have been derived for thermodynamic states where extrema in those properties occur in terms of reduced densities. A possible sound-speed based criterion for refrigeration and power cycle working fluids has been identified.

## Acknowledgement

S.V. and J.A.W. thank financial support by Ministerio de Educación y Ciencia of Spain under Grant FIS2009-07557.

## Appendix A. Supplementary data

Supplementary data associated with this article can be found, in the online version, at <http://dx.doi.org/10.1016/j.jct.2012.07.013>.

## References

- [1] K. Srinivasan, Z. Phys. Chem. 216 (2002) 1379–1388.
- [2] K. Srinivasan, J. Supercrit. Fluids 58 (2011) 26–30.
- [3] G. Bisio, R. Martini, Chem. Eng. Commun. 183 (2000) 207–243.
- [4] K. Srinivasan, P. Sheahen, C.S.P. Sarathy, Int. J. Refrig. 33 (2010) 1395–1401.
- [5] M.F. Taras, A. Lifson, Refrigerant system with intercooler and liquid vapor injection, United States Patent Application Publication No. US 2010 0199694 A1, August 12, 2010.
- [6] R. Zanelli, D. Favrat, Experimental investigation of a hermetic scroll expander-generator, in: International Compressor Engineering Conference, 1994, Paper 1021. <<http://docs.lib.purdue.edu/icec/1021>>.
- [7] H. Wang, R.B. Peterson, T. Herron, Proc. IMechE Part A: J. Power Energy 223 (2009) 863–872.
- [8] S.I. Anisimov, M.I. Tribelsky, Phys. Rev. Lett. 86 (2001) 4037–4040.
- [9] A. Kluwick, Fluid Mech. Appl. 31 (1995) 387–404.
- [10] E.W. Lemmon, M.L. Huber, M.O. McLinden, NIST Standard Reference Database 23: Reference Fluid Thermodynamic and Transport Properties – REFPROP, Version 9.0; Standard Reference Data Program, National Institute of Standards and Technology, Gaithersburg, MD, 390, USA, 2010.
- [11] K. Srinivasan, K.C. Ng, S. Velasco, J.A. White, J. Chem. Thermodyn. 44 (2012) 97–101.
- [12] S. Velasco, J.A. White, K. Srinivasan, P. Dutta, Ind. Eng. Chem. Res. 51 (2012) 3197–3202.
- [13] P. Valentin, R. Balian, A second order equation for deriving the pVT equation of state from the sound velocity with a method to derive the equation itself. <<http://iphf.cea.fr/Docspht/articles/t08/181/public/paperecftp2008Rev1.pdf>>.
- [14] R. Akasaka, Y. Kayukawa, Int. J. Refrig. 35 (2012) 1003–1013.